Fulde-Ferrell-Larkin-Ovchinnikov or Majorana superfluids: The fate of fermionic cold atoms in spin-orbit-coupled optical lattices

Chunlei Qu,[1] Ming Gong,[1,2] and Chuanwei Zhang[1,*]

[1]*Department of Physics, The University of Texas at Dallas, Richardson, Texas 75080 USA*

[2]*Department of Physics and Center of Coherence, The Chinese University of Hong Kong, Shatin, N.T., Hong Kong, China*

(Received 12 June 2013; published 16 May 2014)

The recent experimental realization of spin-orbit (SO) coupling for ultracold atoms opens a completely new avenue for exploring new quantum matters. In experiments, the SO coupling is implemented simultaneously with a Zeeman field. Such SO-coupled Fermi gases are predicted to support Majorana fermions with non-Abelian exchange statistics in one dimension (1D). However, as shown in recent theory and experiments for 1D spin-imbalanced Fermi gases, the Zeeman field can lead to the long-sought Fulde-Ferrell-Larkin-Ovchinnikov (FFLO) superfluids with nonzero center-of-mass momentum Cooper pairings, in contrast to the zero center-of-mass momentum pairings in Majorana superfluids. Therefore a natural question to ask is which phase, FFLO or Majorana superfluids, will survive in SO-coupled Fermi gases in the presence of a large out-of-plane Zeeman field. In this paper, we address this question by studying the mean-field quantum phases of 1D (quasi-1D) SO-coupled fermionic cold-atom optical lattices.

DOI: 10.1103/PhysRevA.89.053618 PACS number(s): 03.75.Ss, 67.85.−d, 74.20.Fg

I. INTRODUCTION

Spin-orbit (SO) coupling plays an important role in many important condensed-matter phenomena [1,2], ranging from spintronics to topological insulators. The recent experimental breakthrough in realizing SO coupling in ultracold Bose and Fermi gases [3–7] provides a new platform for engineering many new many-body quantum matters [8]. In the experiments, the SO coupling is realized together with a Zeeman field. It is well known that such SO coupling and Zeeman field, together with the s-wave superfluid pairing in degenerate Fermi gases, can support zero-energy Majorana fermions [9,10] with non-Abelian exchange statistics when the Zeeman field is beyond a certain critical value [11,12]. In the solid state, the same ingredient has been realized using a heterostructure composed of a semiconductor nanowire (or thin film) with strong SO coupling, an s-wave superconductor, and a magnetic field (or a magnetic insulator) [13–20]. Important experimental progress has been made along this direction [21–24], where some signatures which may be related with Majorana fermions have been observed. In the solid-state heterostructure, the s-wave pairing is induced to the semiconductor through proximity effects [25,26].

In degenerate Fermi gases, however, as observed in both theory and experiments [27–30], the presence of a large Zeeman field (realized by the spin population imbalance) can induce nonzero center-of-mass momentum Cooper pairings between atoms, i.e., Fulde-Ferrell-Larkin-Ovchinnikov (FFLO) phases [31,32], especially in low-dimensional Fermi gases. Such FFLO phases may not support Majorana fermions. Therefore it is natural to ask whether the FFLO superfluids [33–40] with nonzero center-of-mass momentum Cooper pairs or the Majorana superfluids with zero center-of-mass momentum Cooper pairs will survive in the presence of SO coupling and a large out-of-plane Zeeman field. This question becomes especially important because of the recent experimental realization of SO-coupled Fermi gases [6,7], which makes the observation of Majorana fermions in cold atomic systems tantalizingly close. The cold-atom system may be a better platform for the observation of Majorana fermions because of the lack of disorder and impurity [10,37,41–45], an issue that has led to intensive debates in the condensed-matter community on the zero-bias peak signature of Majorana fermions in recent transport experiments [21,22].

In this paper, we address the competition between FFLO and Majorana superfluids by studying the quantum phases of spin-imbalanced Fermi gases in SO-coupled optical lattices. Because the experimentally realized SO coupling is one-dimensional (1D), which is the natural dimension requirement for the realization of Majorana fermions in this system, we consider 1D SO-coupled optical lattices (similar to 1D nanowires) and investigate the quantum phase diagram at zero temperature using the mean-field theory. The quantum phases of Fermi gases are obtained by self-consistently solving the corresponding Bogoliubov–de Gennes (BdG) equation. Without SO coupling, there are no Majorana superfluids, and FFLO superfluids appear in the large-Zeeman-field region. The SO coupling enhances the Majorana superfluid phase while suppressing the FFLO superfluid phase. Majorana and FFLO superfluids exist for different filling factors (i.e., in different chemical-potential regions). We characterize different quantum phases by visualizing their real-space superfluid order parameters, density-of-states distributions, and Majorana zero-energy wave functions. The effects of the harmonic trap are also discussed. We find that similar quantum phases are preserved in a three-dimensional (3D) optical lattice with weak tunneling along the two transversal directions (quasi-1D geometry).

The rest of the paper is organized as follows. In Sec. II, we present the BdG equation for describing Fermi gases in SO-coupled optical lattices. The symmetry of the BdG equation and its effect on the phase diagram is discussed. In Sec. III, we present the main numerical results obtained by self-consistently solving the BdG equation. We discuss the

*chuanwei.zhang@utdallas.edu

phase diagram, the characterization of various phases, and the effects of the harmonic trap and Hartree shift. We also present the results in a 3D optical lattice with weak tunnelings along the two transversal directions. Section IV consists of the discussion and conclusion.

II. HAMILTONIAN AND SYMMETRY

We consider a 1D degenerate Fermi gas with out-of-plane Zeeman field and SO coupling in an optical lattice. The dynamics of this system can be described by the standard tight-binding Hamiltonian

$$\mathcal{H} = \mathcal{H}_0 + \mathcal{H}_Z + \mathcal{H}_{\rm SO}, \tag{1}$$

where the first term is the usual spin-1/2 Fermi-Hubbard model in an optical lattice, which reads

$$\mathcal{H}_0 = -t\sum_{i\sigma}(\hat{c}^\dagger_{i\sigma}\hat{c}_{i+1\sigma} + \text{H.c.}) - \mu\sum_{i\sigma}\hat{n}_{i\sigma} - U\sum_i \hat{n}_{i\uparrow}\hat{n}_{i\downarrow}, \tag{2}$$

where t is the hopping amplitude, μ is the chemical potential, U is the contact interaction ($U > 0$ ensures pairing), and $\hat{n}_{i\sigma} = \hat{c}^\dagger_{i\sigma}\hat{c}_{i\sigma}$, with $\hat{c}_{i\sigma}$ and $\hat{c}^\dagger_{i\sigma}$ being the annihilation and creation operators, respectively. The second and third terms are the out-of-plane Zeeman field

$$\mathcal{H}_Z = -h\sum_i(\hat{c}^\dagger_{i\uparrow}\hat{c}_{i\uparrow} - \hat{c}^\dagger_{i\downarrow}\hat{c}_{i\downarrow})$$

and SO coupling

$$\mathcal{H}_{\rm SO} = \alpha\sum_i(\hat{c}^\dagger_{i-1,\uparrow}\hat{c}_{i\downarrow} - \hat{c}^\dagger_{i+1,\uparrow}\hat{c}_{i\downarrow} + \text{H.c.}),$$

which couples spin-up and -down components of neighboring sites. Such types of SO coupling and Zeeman field have been realized in recent experiments for both bosons and fermions [3–7] using counterpropagating Raman lasers. Note that the wave vector of the Raman lasers determines the strength of the SO coupling α and has no relation to the wave vector of the optical lattice. In experiments, the hopping amplitude, Zeeman field, SO-coupling strength, and contact interactions may be tuned *independently*.

Hereafter in our numerical simulation we set $t = 1$ throughout this work as the basic energy scale. All other energies are scaled by t. The total length of the 1D optical lattice is chosen as $N = 100$, which is long enough to ensure that the coupling between two ends is vanishingly small ($\leqslant 10^{-7}t$). An open boundary condition is used to obtain the zero-energy Majorana fermions at two ends of the 1D optical lattice in the topological superfluid regime.

As the first approach for understanding the quantum phases of such 1D SO-coupled optical lattices, we consider the standard mean-field theory. We decouple the interaction term in $\mathcal{H}_0$ using

$$\begin{aligned}-U\hat{n}_{i\uparrow}\hat{n}_{i\downarrow} = {}& \Delta_i\hat{c}^\dagger_{i\uparrow}\hat{c}^\dagger_{i\downarrow} + \Delta_i^*\hat{c}_{i\downarrow}\hat{c}_{i\uparrow} + |\Delta_i|^2/U \\ & - U\langle\hat{n}_{i\uparrow}\rangle\hat{n}_{i\downarrow} - U\hat{n}_{i\uparrow}\langle\hat{n}_{i\downarrow}\rangle + U\langle\hat{n}_{i\uparrow}\rangle\langle\hat{n}_{i\downarrow}\rangle.\end{aligned} \tag{3}$$

Notice that here we have taken into account the Hartree shift term, which has quantitative effects on our results. The full effective Hamiltonian reads

$$\begin{aligned}\mathcal{H}^{\rm eff} = {}& -t\sum_i\sum_\sigma(\hat{c}^\dagger_{i\sigma}\hat{c}_{i+1\sigma} + \text{H.c.}) - \sum_{i\sigma}\tilde{\mu}_{i\sigma}\hat{c}^\dagger_{i\sigma}\hat{c}_{i\sigma} \\ & + \sum_i(\Delta_i\hat{c}^\dagger_{i\uparrow}\hat{c}^\dagger_{i\downarrow} + \Delta_i^*\hat{c}_{i\downarrow}\hat{c}_{i\uparrow}) + \mathcal{H}_Z + \mathcal{H}_{\rm SO},\end{aligned} \tag{4}$$

where the chemical potential $\tilde{\mu}_{i\sigma} = \mu + U\langle\hat{n}_{i\bar{\sigma}}\rangle$ becomes site dependent, $\bar{\sigma} = -\sigma$. The superfluid pair potential is defined as $\Delta_i = -U\langle\hat{c}_{i\downarrow}\hat{c}_{i\uparrow}\rangle$. Using the Bogoliubov transformation $\hat{c}_{i\sigma} = \sum_n(u^n_{i\sigma}\hat{\Gamma}_n - \sigma v^n_{i\sigma}\hat{\Gamma}^\dagger_n)$ to diagonalize the Hamiltonian into $\mathcal{H}^{\rm eff} = E_g + \sum_n E_n\hat{\Gamma}^\dagger_n\hat{\Gamma}_n$ (where E_g is the ground-state energy and $\hat{\Gamma}^\dagger_n$'s are the quasiparticle creation operators with excitation energy of E_n), we obtain the BdG equation

$$\begin{aligned}&\sum_j\begin{pmatrix} H_{ij\uparrow} & \alpha_{ij} & 0 & \Delta_{ij} \\ -\alpha_{ij} & H_{ij\downarrow} & -\Delta_{ij} & 0 \\ 0 & -\Delta^*_{ij} & -H_{ij\uparrow} & -\alpha_{ij} \\ \Delta^*_{ij} & 0 & \alpha_{ij} & -H_{ij\downarrow}\end{pmatrix}\begin{pmatrix} u^n_{j\uparrow} \\ u^n_{j\downarrow} \\ -v^n_{j\uparrow} \\ v^n_{j\downarrow}\end{pmatrix} \\ &= E_n\begin{pmatrix} u^n_{i\uparrow} \\ u^n_{i\downarrow} \\ -v^n_{i\uparrow} \\ v^n_{i\downarrow}\end{pmatrix},\end{aligned} \tag{5}$$

where $H_{ij\uparrow} = -t\delta_{i\pm1,j} - (\tilde{\mu}_{i\sigma} + h)\delta_{ij}$, $H_{ij\downarrow} = -t\delta_{i\pm1,j} - (\tilde{\mu}_{i\sigma} - h)\delta_{ij}$, $\alpha_{ij} = (j-i)\alpha\delta_{i\pm1,j}$. The other parameters in the above equation can be written as

$$\Delta_{ij} = -U\delta_{ij}\sum_{n=1}^{2N}\left[u^n_{i\uparrow}v^{n*}_{i\downarrow}f(E_n) - u^n_{i\downarrow}v^{n*}_{i\uparrow}f(-E_n)\right], \tag{6}$$

$$\begin{aligned}\langle\hat{n}_{i\uparrow}\rangle &= \sum_{n=1}^{2N}[|u_{i\uparrow}|^2 f(E_n) + |v_{i\uparrow}|^2 f(-E_n)], \\ \langle\hat{n}_{i\downarrow}\rangle &= \sum_{n=1}^{2N}[|u_{i\downarrow}|^2 f(E_n) + |v_{i\downarrow}|^2 f(-E_n)],\end{aligned} \tag{7}$$

with the Fermi-Dirac distribution $f(E) = 1/(1 + e^{E/T})$. The BdG equation (5) should be solved self-consistently with the order-parameter equation (6) and the particle-number equation (7) for the average number of atoms per lattice site $n = \sum_{i,\sigma}\langle\hat{n}_{i\sigma}\rangle/N$. Here we denote n as the filling factor for convenience. In our simulation, we take the attractive interaction strength $U = 4.5t$ and the temperature $T = 0$.

The original Hamiltonian Eq. (1) contains no imaginary part; therefore the wave function in Eq. (5) can be made real, and the order parameter in Eq. (4) is also real. This 1D or quasi-1D system preserves an additional chiral symmetry, which is broken in a two-dimensional (2D) Rashba SO-coupling system. According to the topological classification [46], our effective model belongs to the BDI symmetry class (which is characterized by an integer $\mathbb{Z}$ topological invariant) instead of the D class, which has a $\mathbb{Z}_2$ topological invariant in 1D [41,47,48]. The integer invariant $\mathbb{Z}$ indicates the number of zero-energy Majorana fermions at each end of the 1D system, as we will show in Sec. III D that our quasi-1D system does host multiple Majorana fermions. The mean-field Hamiltonian (4) still preserves the basic symmetry properties

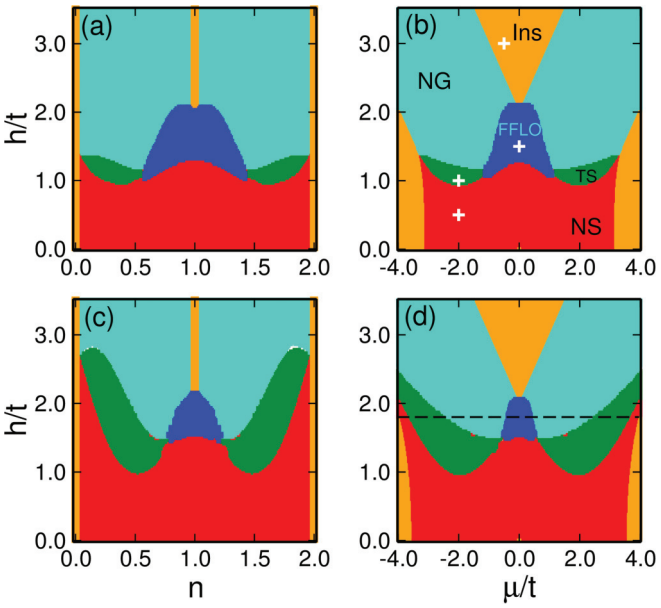

FIG. 1. (Color online) Phase diagram of 1D SO-coupled optical lattices as a function of Zeeman field h and (a) and (c) filling factor n or (b) and (d) chemical potential μ. (top) SO coupling $\alpha = 0.5t$; (bottom) $\alpha = 1.0t$. Five different phases are identified in each phase diagram: normal BCS superfluid (NS), topological superfluid (TS), FFLO, normal gas (NG), and insulator phase (Ins).

of Eq. (1). Consider the particle-hole operation

$$\mathcal{C}\begin{pmatrix}\hat{c}_{i\uparrow}\\ \hat{c}_{i\downarrow}\end{pmatrix}\mathcal{C}^{-1} = (-1)^i\begin{pmatrix}\hat{c}^\dagger_{i\uparrow}\\ \hat{c}^\dagger_{i\downarrow}\end{pmatrix}; \tag{8}$$

we have $\mathcal{C}H(\mu)\mathcal{C}^{-1} = H(-\mu)$ when the Hartree shift term is ignored and $\mathcal{C}H(\mu)\mathcal{C}^{-1} = H(-U-\mu)$ when the Hartree shift term is included. Thus the spectrum should be symmetric about $\mu = 0$ without Hartree shift and $\mu = -\frac{U}{2}$ with Hartree shift in Eq. (4), which is confirmed in our numerical results (see Figs. 1 and 6). However, in the presence of a trapping potential, the chemical potential becomes site dependent; thus the particle-hole symmetry $\mathcal{C}$ is broken, and the band structure is no longer symmetric about $\mu = 0$. We emphasize that this particle-hole symmetry is a particular symmetry for a lattice system with respect to half filling and should not be confused with the inherent particle-hole symmetry of the BdG Hamiltonian, which is used for topological classifications.

III. PHASE DIAGRAM: MAJORANA VERSUS FFLO SUPERFLUIDS

We self-consistently solve the BdG equations (5), (6), and (7) with an open boundary condition to obtain the phase diagram. The SO-coupled optical lattice supports several different phases: normal BCS superfluid (NS) with $\Delta \neq 0$ and all nonzero quasiparticle excitation energies, topological superfluids with $\Delta \neq 0$ and zero-energy Majorana fermions located at two ends of the lattice, FFLO phase with oscillating Δ and magnetization, insulator phase (Ins) with integer filling factor and finite-energy gaps, and normal gas (NG) phase without pairing and energy gap. These properties allow us to identify the five distinct phases without any ambiguity. We first study the phases without Hartree shift and address the role of Hartree shift later.

A. Phase diagram without Hartree shift

Our numerical results are presented in Fig. 1 for two different sets of SO-coupling strength. In Figs. 1(a) and 1(c) we plot the phase diagram in the h-n plane, and in Figs. 1(b) and 1(d) we plot the results in the h-μ plane. We see the phase diagram is symmetric around $n = 1$ or $\mu = 0$, as discussed in the previous section. When the Zeeman field h is very small, the system favors the normal BCS superfluids. With increasing Zeeman field h, topological superfluids and FFLO phases emerge as the ground states of the system for different filling factors. The FFLO phase is more likely to be observed around the integer filling factor $n = 1$. When the Zeeman field becomes even larger, where only atoms with one type of spin can stay on each lattice site, the insulator phase develops with the filling factor $n = 1$. The insulator phase can also be found when μ is too large (fully occupied band) or to small (empty band). The topological phase and associated Majorana fermions emerge with fractional filling factors n. By comparing the phase region for different SO couplings, we find that the SO coupling enhances the topological superfluid phase and suppresses the FFLO phase. Note that without SO coupling, there is only the FFLO phase and no topological superfluid phase [27,29].

Different quantum phases in Fig. 1 can be characterized by different densities of states (DOS) $\rho(E) = \sum[|u_{i\sigma}|^2\delta(E - E_n) + |v_{i\sigma}|^2\delta(E + E_n)]$ as a function of energy E and superfluid order parameter $\Delta(x_i) = \Delta_i$, as shown in Fig. 2. In

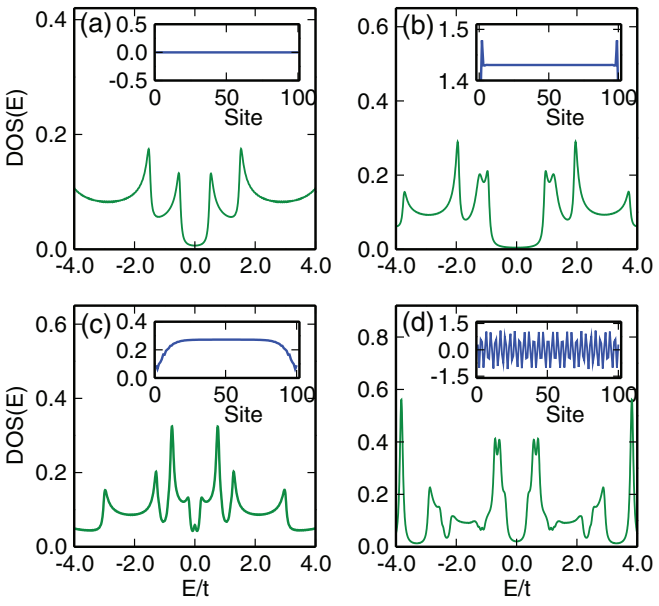

FIG. 2. (Color online) Representative density of states for (a) the insulator phase, (b) normal BCS superfluid phase, (c) topological superfluid phase, and (d) FFLO phase. The insets show the order parameters in each phase. The corresponding phase points are marked by the plus signs in Fig. 1(b). Note that there is a zero-energy peak in the DOS in the topological superfluid phase as shown in (c).

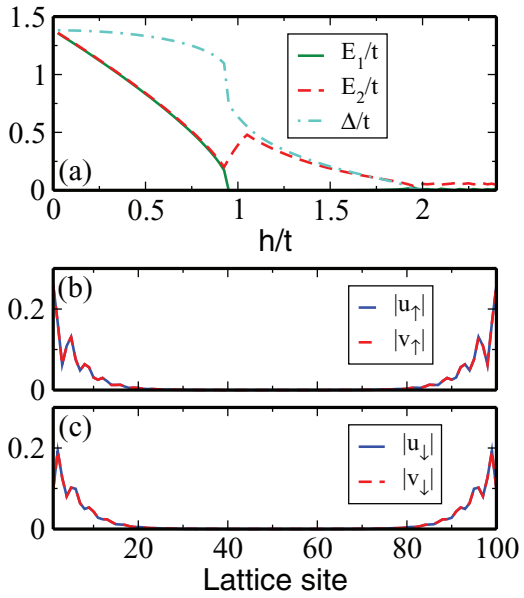

FIG. 3. (Color online) (a) Plot of the order parameter and the two lowest eigenenergies E_1 and E_2 as a function of Zeeman field for the transition from normal BCS superfluids to topological superfluids. $\alpha = 1.0t, \mu = -2.0t$. (b) and (c) The Majorana zero-energy-state wave function.

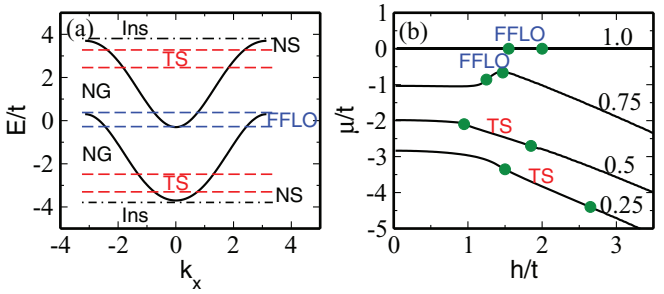

FIG. 4. (Color online) Single-particle band structure of the SO-coupled optical lattices. $\alpha = 1.0t$, $h = 1.7t$ [corresponding to the dashed line in Fig. 1(d)]. The corresponding chemical-potential regions for different phases are identified. (b) Plot of μ as a function of Zeeman field for fixed filling factor $n = 0.25, 0.5, 0.75, 1.0$. The regions between the two circles on each line label the topological superfluid phase (for $n = 0.25, 0.5$) or the FFLO phase (for $n = 0.75, 1.0$).

the insulator phase [Fig. 2(a)], the order parameter $\Delta = 0$, and there is an energy gap for excitations. In the normal BCS superfluid phase [Fig. 2(b)], the order parameter is nonzero, and there is a superfluid gap around $E = 0$. In the topological superfluid phase [Fig. 2(c)], a zero-energy peak appears in the DOS which corresponds to the zero-energy Majorana fermions. Note that for the normal BCS superfluid phase the order parameter has a strong oscillation near each end, while for the topological superfluid, the order parameter is a monotonic function of the sites. Similar features have always been found for these two different phases for different parameters. The FFLO phase [Fig. 2(d)] is characterized by the spatially oscillating order parameter, and the excitations are always gapless.

The emergence of a Majorana zero-energy state at the ends of the SO-coupled optical lattices can clearly be seen in Fig. 3. In Fig. 3 we plot the average order parameter $\Delta = \sum_i |\Delta|_i / N$ and the first and second non-negative eigenvalues, denoted by E_1 and E_2, of the BdG equation as a function of Zeeman field. We see that in the normal BCS superfluid regime E_1 is always equal to E_2 and smaller than the order parameter. The energy gap not equal to the order parameter is a unique feature for SO-coupled systems. When h approaches $1.0t$ ($h > \Delta$), we observe a sudden jump of the order parameter, and the system enters the topological superfluid regime, where $E_1 = 0$, and E_2 increases and reaches the maximum value 0.5 at $h \sim 1.1t$. When h further increases, $E_2 \sim \Delta$ gradually decreases and becomes zero when the system enters the normal gas phase. In the topological superfluid phase, E_2 is the minimum energy gap that protects the topological zero-energy Majorana state. In Figs. 3(b) and 3(c), we plot the zero-energy state, which is the eigenstate of the Bogoliubov quasiparticle operators $\hat{\Gamma}_0^\dagger = \sum_{i\sigma}(u_{i\sigma}^0 \hat{c}_{i\sigma}^\dagger + v_{i\sigma}^0 \hat{c}_{i\sigma})$. The eigenstate satisfies the condition that $u_{i\sigma} = v_{i\sigma}$ on one end and $u_{i\sigma} = -v_{i\sigma}$ on the other end. Thus, by defining $\hat{\Gamma}_0^\dagger = \gamma_L + i\gamma_R$, we could identify the left- and right-end Majorana fermions $\gamma_{L(R)}$.

The emergence of different phases in different parameter regions can be understood intuitively from the single-particle band structure (e.g., Fig. 4). When the Zeeman field is very small, the pairing between atoms on the same Fermi surface is preferred, and this is the normal BCS superfluid; for a larger Zeeman field, depending on the filling factor or the chemical potential, two intriguing new phases appear: topological BCS superfluids and FFLO superfluids. In the topological BCS superfluids, the chemical potential cuts either the lower band (the higher band is empty) or the higher band (the lower band is well below the Fermi surface), and pairings between different bands are not allowed, leading to an effective p-wave pairing that can host Majorana fermions. In this region, Cooper pairings occurring near the Fermi surface have zero center-of-mass momentum. Near half filling, both bands are partially occupied, and there is a competition between intraband pairing (BCS) and interband pairing (FFLO). The latter dominates when the Zeeman field is relatively large, leading to FFLO superfluids near the half filling. Generally, whether we have BCS or FFLO superfluids, the Cooper pairings can be destroyed by a strong enough external Zeeman field, and the system eventually evolves into a normal gas phase. An exception occurs at exactly half filling ($n = 1$), where the lower band is fully occupied and there is a finite-energy gap between the two bands, corresponding to an insulator phase.

As an example, in Fig. 4 we plot the band structure for $\alpha = 1.0t$, $h = 1.7t$, which corresponds to the dashed line in Fig. 1(d). The chemical-potential regions for different phases are identified. Note that without SO coupling, the system is a normal gas or insulator for such a large Zeeman field. The appearance of superfluids is due to the presence of SO coupling $2\alpha \sin(k_x)\sigma_y$, which mainly modifies the band structure around the edge ($k_x \approx \pm\pi$) and bottom ($k_x \approx 0$) of each band in a way similar to a linear SO coupling. Therefore the superfluids are sustained only at very low filling factors (band bottom) or half-filling factors (band edge), and we see BCS (nontopological

or topological) superfluids and FFLO superfluids appear at two sides of the normal gas in each band for such a large Zeeman field. The topological superfluids appear when the chemical potential cuts either the lower or the upper band, and FFLO superfluids appear near half filling, in agreement with the above analysis.

Because of the SO coupling, the spin polarization is not a conserved quantity anymore, which is different from the spin-imbalanced Fermi gases in the literature. However, the filling factor can still be controlled precisely in experiments. With increasing Zeeman field, the chemical potential changes for a fixed filling factor, leading to the transition between different phases. In Fig. 4(b) we plot the chemical potential as a function of Zeeman field for different filling factors n. Generally, when $n < 0.7$ or $n > 1.3$, we find μ changes monotonically as a function of the Zeeman field. However, in the case $n = 0.75$, the chemical potential does not change when $h < 1.0t$ and then increases slightly when the system enters the FFLO phase regime. For $n = 1$, the chemical potential is independent of the filling factor due to the particle-hole symmetry. Notice that n is not a simple function of the chemical potential; therefore in Fig. 1 we see that the FFLO phase is very large in the h-n plane but becomes much smaller in the h-μ plane.

B. Phase diagram in a harmonic trap

In a realistic experiment, a harmonic trapping potential $V(x_i) = \frac{1}{2}\omega_x^2(i - L_c)^2$ exists, where ω_x is the trapping frequency and L_c is the center of the lattice. The effects of the trapping potential on the order parameter and filling factor are shown in Figs. 5(a) and 5(b). With increasing trapping frequency, the ultracold atoms are forced to the center of the trap, which has a lower potential. With a high trapping frequency, a shell structure is developed, where superfluid, insulator, and normal gas phases appear in different regions of the harmonic trap. Different phases in different regions can be understood based on the local-density approximation where the local chemical potential $\mu(x_i) = \mu_c - V(x_i)$, where μ_c is the chemical potential at the trap center. As shown in Figs. 5(a) and 5(b), without a trap, the order parameters are uniform in the bulk, and the filling factor is about 0.475; this is in the topological phase region. With the increase of the trapping frequency, the particles accumulate in the center of the trap, as shown in Fig. 5(b). For very large trapping frequency $\omega_x = 0.2$, there are no atoms except in a small region around the trap center. The order parameter vanishes because of the vacuum state on the edges and the normal gas phase in the trap center [blue dash-dotted line in Figs. 5(a) and 5(b)]. For other medium values of the trapping frequency, more different phases mix and could not be identified. In the superfluid regime in the trap, a topological superfluid or FFLO phase may develop for different parameters. In Figs. 5(c) and 5(d) we plot the phase diagram for a fixed trapping potential. Notice that there is always a mixture of different phases in different regions of the trap depending on their local chemical potentials; therefore we only identify three different phases in our plot: normal gas for the whole lattice, topological superfluids (with zero-energy Majorana fermions), and other superfluids (normal BCS superfluids or FFLO) in a certain part of the lattice. In the topological superfluid, the Majorana

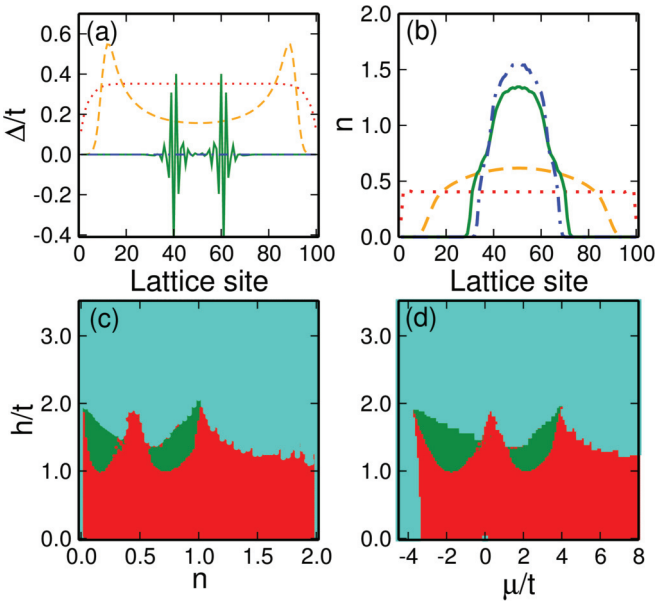

FIG. 5. (Color online) Phase diagram in the presence of a harmonic trap. (a) Order parameter profiles and (b) atom density distributions for different trapping frequencies: $\omega_x = 0.0$ (red dotted line), 0.05 (orange dashed line), 0.15 (green solid line), and 0.2 (blue dash-dotted line). In (a) and (b), we fix the Zeeman field $h = 1.0t$ and the average filling factor $n = 0.475$. (c) and (d) are phase diagrams as a function of Zeeman field h and filling factor n or chemical potential μ. In all the plots, $\alpha = 1.0t$.

zero-energy states do not localize at the two ends of the trap but in a certain middle region of the trapping potential [38]. The position of the Majorana fermions changes with the trapping frequency. With the presence of a trapping potential, the effective chemical potential is site dependent; therefore the particle-hole symmetry for lattices is broken, and the phase diagram is not symmetric with respect to half filling $n = 1$ [Fig. 5(c)] or $\mu = 0$ [Fig. 5(d)].

C. Effect of Hartree shift

We also study the effect of the Hartree shift on the phase diagram. When the Hartree shift is included, the local chemical potential and Zeeman field are both modified, as seen from $\tilde{\mu}_{i\sigma} = \mu + U\langle\hat{n}_{i\bar{\sigma}}\rangle$. If we define $\langle\hat{n}_i\rangle$ and $\langle\hat{m}_i\rangle$ as the local particle number and magnetization $m_i = n_{i\uparrow} - n_{i\downarrow}$, then the modified chemical potential and Zeeman field when including the Hartree shift term will be $\mu_i = \mu + U\langle\hat{n}_i\rangle$ and $h_i = h - \frac{U}{2}\langle\hat{m}_i\rangle$. The numerical results are presented in Fig. 6 for a direct comparison with the results without Hartree shift [Figs. 1(c) and 1(d)]. Here the topological phase can be determined based on the modified chemical potential and Zeeman field. We see the phase diagram is still qualitatively the same except that now the phase diagram is symmetric for $\mu = -U/2$, as discussed above. Since the Zeeman field h_i depends strongly on the local magnetization m_i and the FFLO phase is a competition between superfluid and magnetization, it is hard to numerically determine FFLO phases near the phase boundary between FFLO and topological superfluid phases. This is because the total free energy becomes extremely

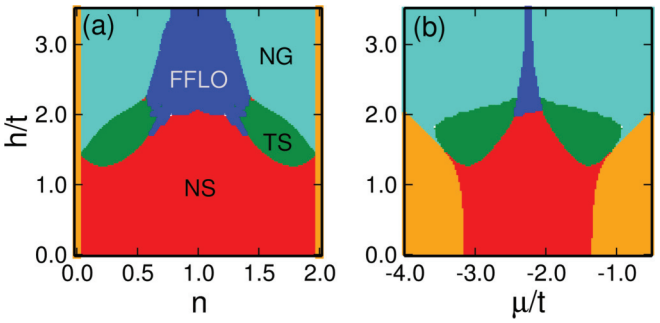

FIG. 6. (Color online) Phase diagram with the inclusion of the Hartree shift. $\alpha = 0.5t$. All other parameters and notations are the same as those in Fig. 1.

complex as a function of the order parameters and other quantities, and most solutions we find correspond to excited states, instead of the global minimum of the free energy. Thus the boundary between the topological superfluid and FFLO phase cannot be determined precisely.

D. Quantum phases in quasi-1D lattices

In a truly 1D system, quantum fluctuations become significant and need to be taken into account, which is beyond our mean-field approximation. The quantum fluctuations can be suppressed by considering a three-dimensional lattice with weak coupling $t_\perp = 0.1t$ along two transversal directions, similar to the high-temperature cuprate superconductor where the 2D superconductivity is stabilized by weak coupling along the third direction. In experiments, such a setup can be realized in 3D degenerate Fermi gases subject to 2D strong optical lattices, forming weakly coupled 1D tubes. The 1D weak lattice and SO coupling are then applied on each tube. The quantum phases in the quasi-1D system are calculated by self-consistently solving the corresponding BdG equation and are found to be similar to the above 1D results. Here we focus on the interesting topological and FFLO phases. The order parameters of these two phases in quasi-1D lattices are shown in Figs. 7(a) and 7(b). Compared to the 1D results, the order parameters only change slightly due to the week tunneling between neighboring tubes. In contrast to the 1D lattices, the array of lattice tubes can host multiple Majorana zero-energy states at each end, as shown in Fig. 7(c) for the Bogoliubov excitation spectrum. This verifies that our system belongs to the BDI topological class which has an integer topological invariant $\mathbb{Z}$ [47]. The weak tunnelings do not lift the zero-energy degeneracy because there is no SO coupling along the transversal directions and the chemical potential cuts all the subbands, which is in sharp contrast to the case with Rashba SO coupling, where zero-energy states only survive for an odd number of lattice tubes [49]. In our case, the zero-energy wave functions are still localized around the edges of the tubes but can expand along the transversal directions due to the weak tunneling, as shown in Fig. 7(d). Note that each of these nine zero-energy states does not distribute evenly over the nine tubes. Although the wave functions of the edge modes are mixed together, their direct couplings between zero-energy states are forbidden by the chiral symmetry. The number of

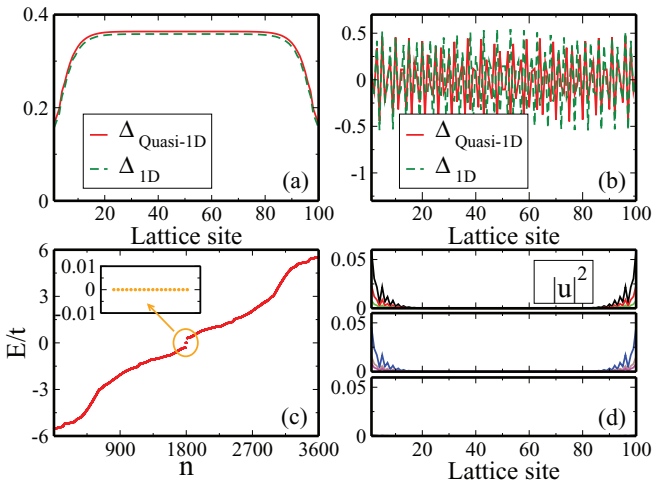

FIG. 7. (Color online) Topological and FFLO phases in quasi-1D ($100 \times 3 \times 3$) lattices. The order parameters in (a) topological superfluid and (b) FFLO phases. Red solid lines: quasi-1D; green dashed lines: 1D for the same parameters. (c) The BdG excitation spectrum in the topological superfluid phase. The inset shows the nine zero-energy states (18 zero energies total shown due to the intrinsic particle-hole symmetry of the BdG equation). (d) The corresponding edge-state wave function along nine tubes (denoted by different colors) of the quasi-1D lattice for one of the zero-energy states. Because of the weak transversal tunneling, each of the nine zero-energy states expands but is distributed unevenly over the nine tubes. Other parameters are $h = 1.2t$, $\mu = -2t$ for the topological superfluid phase and $h = 1.8t$, $\mu = 0$ for the FFLO phase.

zero-energy Majorana fermions may change with increasing transversal tunneling strength whenever the subband splitting is larger than the Zeeman splitting [50].

IV. DISCUSSION AND CONCLUSION

By considering 1D Fermi gases without the lattice, a direct phase transition from FFLO superfluids to Majorana superfluids with increasing SO coupling was briefly discussed for one fixed Zeeman field and density [38]. Such a direct transition may not occur for general Zeeman field and density, where other phases (normal gas, BCS superfluids, etc.) may appear in the transition, as shown in our lattice system. In a lattice system, the filling factor has a direct physical meaning: at each lattice site, there are at most two fermions. Our results mainly focus on the change in the quantum phase diagrams with filling factors and Zeeman fields in the lattice. The phase diagram and its physical interpretation provide direct knowledge on why it is impossible to find the coexistence of topological and FFLO phases in such a system in the presence of a large Zeeman field. It is also more natural to generalize the 1D lattice results to weakly coupled quasi-1D systems than the 1D continuous system.

Two intriguing phases can be detected in realistic experiments. Signatures of Majorana superfluids and FFLO superfluids have been proposed separately in cold atoms. For instance, the finite center-of-mass momentum of Cooper pairings of the FFLO superfluids can be detected by the noise correlation of

the time-of-flight images [51]. In the topological phase, the spatially localized Majorana fermions can be detected using spatially resolved radio-frequency spectroscopy [52].

In summary, in this paper, we address the question of which phase, FFLO or Majorana superfluids, will survive in SO-coupled Fermi gases in the presence of a large out-of-plane Zeeman field by studying the mean-field quantum phases of the 1D and quasi-1D SO-coupled optical lattices. In the optical lattice system each site can host at most two fermions, making the system host plenty of phases depending on the filling factor and the Zeeman field, which is quite different from the free-space results. At a finite Zeeman field we observe strong competition between the topological superfluid phase and FFLO phase. The SO coupling enhances the topological superfluid phase while suppressing the FFLO phase. The weak tunneling along transversal directions in quasi-1D lattices does not change the results. These results not only are important for searching for Majorana fermions in SO-coupled degenerate Fermi gases but may also have significant applications for the solid-state nanowire heterostructures where a similar physics exists.

ACKNOWLEDGMENTS

C.Q. and C.Z. are supported by ARO (Grant No. W911NF-12-1-0334), AFOSR (Grant No. FA9550-13-1-0045), and NSF-PHY (Grant No. 1249293). M.G. is supported by Hong Kong RGC/GRF Projects (No. 401011 and No. 2130352), University Research Grant (No. 4053072), and The Chinese University of Hong Kong (CUHK) Focused Investments Scheme.

[1] M. Z. Hasan and C. L. Kane, Rev. Mod. Phys. **82**, 3045 (2010).
[2] X.-L. Qi and S.-C. Zhang, Rev. Mod. Phys. **83**, 1057 (2011).
[3] Y.-J. Lin, K. Jiménez-García, and I. B. Spielman, Nature (London) **471**, 83 (2011).
[4] J. Y. Zhang, S. C. Ji, Z. Chen *et al.*, Phys. Rev. Lett. **109**, 115301 (2012).
[5] C. Qu, C. Hamner, M. Gong, C. Zhang, and P. Engels, Phys. Rev. A **88**, 021604(R) (2013).
[6] P. Wang, Z.-Q. Yu, Z. Fu, J. Miao, L. Huang, S. Chai, H. Zhai, and J. Zhang, Phys. Rev. Lett. **109**, 095301 (2012).
[7] L. W. Cheuk, A. T. Sommer, Z. Hadzibabic, T. Yefsah, W. S. Bakr, and M. W. Zwierlein, Phys. Rev. Lett. **109**, 095302 (2012).
[8] V. Galitski and I. B. Spielman, Nature (London) **494**, 49 (2013).
[9] C. Zhang, S. Tewari, R. M. Lutchyn, and S. Das Sarma, Phys. Rev. Lett. **101**, 160401 (2008).
[10] M. Sato, Y. Takahashi, and S. Fujimoto, Phys. Rev. Lett. **103**, 020401 (2009).
[11] A. Kitaev, Ann. Phys. (N.Y.) **303**, 2 (2003).
[12] C. Nayak, S. H. Simon, A. Stern, M. Freedman, and S. Das Sarma, Rev. Mod. Phys. **80**, 1083 (2008).
[13] L. Fu and C. L. Kane, Phys. Rev. Lett. **100**, 096407 (2008).
[14] J. D. Sau, R. M. Lutchyn, S. Tewari, and S. Das Sarma, Phys. Rev. Lett. **104**, 040502 (2010).
[15] J. D. Sau, S. Tewari, R. Lutchyn, T. Stanescu, and S. Das Sarma, Phys. Rev. B **82**, 214509 (2010).
[16] J. Alicea, Phys. Rev. B **81**, 125318 (2010).
[17] R. M. Lutchyn, J. D. Sau, and S. Das Sarma, Phys. Rev. Lett. **105**, 077001 (2010).
[18] Y. Oreg, G. Refael, and F. von Oppen, Phys. Rev. Lett. **105**, 177002 (2010).
[19] A. C. Potter and Patrick A. Lee, Phys. Rev. Lett. **105**, 227003 (2010).
[20] L. Mao, M. Gong, E. Dumitrescu, S. Tewari, and C. Zhang, Phys. Rev. Lett. **108**, 177001 (2012).
[21] V. Mourik, K. Zuo, S. M. Frolov S. Tewari, and C. Zhang, Science **336**, 1003 (2012).
[22] A. Das, Y. Ronen, Y. Most, Y. Oreg, M. Heiblum, and H. Shtrikman, Nat. Phys. **8**, 887 (2012).
[23] M. T. Deng, C. L. Yu, G. Y. Huang, M. Larsson, P. Caroff, and H. Q. Xu, Nano Lett. **12**, 6414 (2012).
[24] L. P. Rokhinson, X. Liu, and J. K. Furdyna, Nat. Phys. **8**, 795 (2012).
[25] Y.-J. Doh, J. A. van Dam, A. L. Roest, E. P. A. M. Bakkers, L. P. Kouwenhoven, and S. D. Franceschi, Science **309**, 272 (2005).
[26] J. Xiang, A. Vidan, M. Tinkham, R. M. Westervelt, and C. M. Lieber, Nat. Nanotechnol. **1**, 208 (2006).
[27] M. R. Bakhtiari, M. J. Leskinen, and P. Torma, Phys. Rev. Lett. **101**, 120404 (2008).
[28] M. M. Parish, S. K. Baur, E. J. Mueller, and D. A. Huse, Phys. Rev. Lett. **99**, 250403 (2007).
[29] Y. L. Loh and N. Trivedi, Phys. Rev. Lett. **104**, 165302 (2010).
[30] Y.-A. Liao, A. S. C. Rittner, T. Paprotta, W. Li, G. B. Partridge, R. G. Hulet, S. K. Baur, and E. J. Mueller, Nature (London) **467**, 567 (2010).
[31] P. Fulde and R. A. Ferrell, Phys. Rev. **135**, A550 (1964).
[32] A. I. Larkin and Yu. N. Ovchinnikov, Zh. Eksp. Teor. Fiz. **47**, 1136 (1964) [Sov. Phys. JETP **20**, 762 (1965)].
[33] M. Iskin, Phys. Rev. A **86**, 065601 (2012).
[34] Z. Zheng, M. Gong, X. Zou, C. Zhang, and G.-C. Guo, Phys. Rev. A **87**, 031602(R) (2013).
[35] X.-J. Liu and H. Hu, Phys. Rev. A **87**, 051608(R) (2013).
[36] L. Dong, L. Jiang, and H. Pu, New J. Phys. **15**, 075014 (2013).
[37] X.-J. Liu, L. Jiang, H. Pu, and H. Hu, Phys. Rev. A **85**, 021603(R) (2012).
[38] X.-J. Liu and H. Hu, Phys. Rev. A **85**, 033622(R) (2012).
[39] F. Wu, G.-C. Guo, W. Zhang, and W. Yi, Phys. Rev. Lett. **110**, 110401 (2013).
[40] Y. Xu, C. Qu, M. Gong, and C. Zhang, Phys. Rev. A **89**, 013607 (2014).
[41] X. J. Liu, Z. X. Liu, and M. Cheng, Phys. Rev. Lett. **110**, 076401 (2013).
[42] L. Jiang, T. Kitagawa, J. Alicea, A. R. Akhmerov, D. Pekker, G. Refael, J. I. Cirac, E. Demler, M. D. Lukin, and P. Zoller, Phys. Rev. Lett. **106**, 220402 (2011).
[43] M. Gong, S. Tewari, and C. Zhang, Phys. Rev. Lett. **107**, 195303 (2011).
[44] M. Gong, G. Chen, S. Jia, and C. Zhang, Phys. Rev. Lett. **109**, 105302 (2012).

[45] S. L. Zhu, L. B. Shao, Z. D. Wang, and L. M. Duan, Phys. Rev. Lett. **106**, 100404 (2011).
[46] A. P. Schnyder, S. Ryu, A. Furusaki, and A. W. W. Ludwig, Phys. Rev. B **78**, 195125 (2008).
[47] S. Tewari and J. D. Sau, Phys. Rev. Lett. **109**, 150408 (2012).
[48] S. Tewari, T. D. Stanescu, J. D. Sau, and S. Das Sarma, Phys. Rev. B **86**, 024504 (2012).
[49] T. Mizushima and M. Sato, New J. Phys. **15**, 075010 (2013).
[50] C. Qu, M. Gong, Y. Xu, S. Tewari, and C. Zhang, arXiv:1310.7557.
[51] M. Greiner, C. A. Regal, J. T. Stewart, and D. S. Jin, Phys. Rev. Lett. **94**, 110401 (2005).
[52] Y. Shin, C. H. Schunck, A. Schirotzek, and W. Ketterle, Phys. Rev. Lett. **99**, 090403 (2007).